

Synthesis and Characterization of the Gold Nanoparticle/SU-8 Nanocomposite Material

Anju Toor



Electrical Engineering and Computer Sciences
University of California at Berkeley

Technical Report No. UCB/EECS-2016-34

<http://www.eecs.berkeley.edu/Pubs/TechRpts/2016/EECS-2016-34.html>

May 1, 2016

Copyright © 2016, by the author(s).
All rights reserved.

Permission to make digital or hard copies of all or part of this work for personal or classroom use is granted without fee provided that copies are not made or distributed for profit or commercial advantage and that copies bear this notice and the full citation on the first page. To copy otherwise, to republish, to post on servers or to redistribute to lists, requires prior specific permission.

**Synthesis and Characterization of the Gold Nanoparticle/SU-8
Nanocomposite Material**

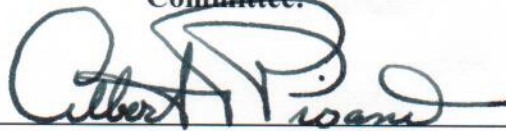
Anju Toor

Research Project

Submitted to the Department of Electrical Engineering and Computer Sciences,
University of California at Berkeley, in partial satisfaction of the requirements for the
degree of **Master of Science, Plan II.**

Approval for the Report and Comprehensive Examination:

Committee:



Professor Albert P. Pisano
Research Advisor

13 MAY 2015

(Date)



Professor Liwei Lin
Second Reader

5/13/2015

Synthesis and Characterization of the Gold Nanoparticle/SU-8 Nanocomposite Material

by

Anju Toor

BE (University of Delhi, India) 2010

A report submitted in partial satisfaction of the
requirements for the degree of

Masters of Science, Plan II

in

Electrical Engineering and Computer Sciences

at the

University of California at Berkeley

Committee in Charge:

Professor Albert P. Pisano, Chair

Professor Liwei Lin

Spring 2015

Synthesis and Characterization of the Gold Nanoparticle/SU-8 Nanocomposite Material

Copyright © 2015

by

Anju Toor

Abstract

Synthesis and Characterization of the Gold Nanoparticle/SU-8 Nanocomposite Material

by

Anju Toor

Masters of Science, Plan II in Electrical Engineering and Computer Sciences

University of California, Berkeley

Professor Albert P. Pisano, Chair

Polymer nanocomposite materials containing inorganic fillers such as metallic particles dispersed in a polymer have been the subject of intense research because of their enormous potential as electronic, photonic and energy storage materials. These hybrid materials combine the functionality of nanoparticles with the processability of polymer films. However, in order to achieve optimal performance of the composite material a uniform dispersion of nanoparticles is necessary to fully utilize the properties of nanoparticles. Usually the dispersion of nanoparticles in polymers is challenging and the nanoparticles tend to agglomerate or/and phase separate in the host polymer matrix [1].

In this study, (1) a novel nanocomposite material containing dodecanethiol functionalized gold nanoparticle (5 nm in diameter) fillers and SU-8 epoxy resin as the host polymer and (2) a film casting method to reduce the number of voids and cracks through the nanocomposite film were developed. Effect of dodecanethiol ligand on particle agglomeration and dispersion in the SU-8 host matrix will be examined. Nanocomposite film morphology and chemical composition will be discussed. Characterization of the dielectric properties (effective dielectric constant and loss tangent) of the polymer nanocomposite will also be discussed.

To my family, and those who are like family

Acknowledgments

First of all, I would like to express my deepest appreciation to my advisor, Prof. Albert P. Pisano, for his support and guidance. He provided insightful comments and suggestions during our research discussions. He also gave me the freedom to follow my own research interests. He provided every opportunity to present my work to other researchers in the field through conferences and research exhibitions. Thank you for providing me the opportunity to pursue my graduate studies under your supervision. I would also like to thank Prof. Liwei Lin for agreeing to be the reader of this research report.

I owe my sincere gratitude to Dr. Jim Cheng who served as a mentor and provided invaluable guidance. I enjoyed my stimulating research discussions with him. Several peers in the Pisano Research for Integrated Micromechanical and Electrical (PRIME) Systems Laboratory including Dr. Mitsutoshi Makihata, Dr. Kristen Dorsey, Kirti Mansukhani, Nuo Zhang, Hongyun So, Lilla Smith and David Rolfe have been helpful throughout the research by providing me with their discerning feedback and support. I would also like to thank my friend Animesh Garg for his support and never ending faith in my capabilities. Finally, I would like to thank my parents for their never ending love and continuous support. Without their encouragement and support, I could not have make my dream of studying abroad come true.

Contents

Contents	iv
List of Figures	v
List of Tables	vii
1 Nanocomposites	1
1.1 Introduction and Background	1
1.2 Contribution	2
2 Experimental Details	4
2.1 Materials	4
2.2 Nanocomposite Processing & Characterization Methods	7
3 Material Characterization	10
3.1 Scanning Electron Microscopy	10
3.2 Energy Dispersive X-Ray Spectroscopy	13
3.3 Transmission Electron Microscopy	15
3.4 Discussion	18
4 Electrical Characterization	19
4.1 Device Fabrication	19
4.2 Measurements & Results	20
4.3 Discussion	23
5 Conclusion and Future Work	24
5.1 Conclusion	24
5.2 Future Work	24
References	26

List of Figures

1.1	Schematic to show a ligand capped nanoparticle surface	2
2.1	Molecular structure of SU-8 monomer. There are eight epoxy groups in the monomer, which justifies the number '8' in the name (SU-8). [21].	6
2.2	Chemical structure of dodecanethiol ligand. Dodecanethiol is a long carbon chain (12C atoms), with a sulphur atom that binds covalently to the metal nanoparticle core [22].	7
2.3	<i>Ex situ</i> method of polymer nanocomposite material synthesis. In this technique, nanoparticle and polymer components are synthesized separately and then blended to prepare the nanocomposite material.	7
3.1	Various steps involved in the synthesis of nanocomposite film. After spin coating the nanocomposite film, it is soft-baked to allow evaporation of solvent. Next, it is exposed to UV light for a certain time which depends on the nanocomposite film thickness followed by a hard bake step, to polymerize the SU-8 in the nanocomposite film. . . .	11
3.2	SEM image of the top surface of drop-casted nanocomposite film (sample-1). As evident from the presence of microbubbles and voids, a porous nanocomposite film is obtained.	11
3.3	Cross-section of the nanocomposite film obtained from sample-2. Unlike sample-1, there are no voids through the nanocomposite film, but a thicker film is obtained ($\sim 65 \mu m$).	12
3.4	SEM image of the top surface of the spin-coated nanocomposite film (sample-3). There are few voids but overall a dense film is obtained.	12
3.5	EDX analysis of the gold nanoparticle/SU-8 polymer composite material. Figure 3.5 (a) corresponds to the SEM image of the top surface of nanocomposite film. The individual elemental maps are shown in Figure 3.5 (b-d). These maps reveal that C, O and Au are the elemental constituents of the nanocomposite film. Further, the elemental map of Au qualitatively suggests a homogeneous dispersion of gold nanoparticles in the polymer matrix.	14
3.6	TEM image of dodecanethiol functionalized gold nanoparticles	16
3.7	TEM analysis of the drop-casted nanocomposite films. These images show that nanoparticles are dispersed in form of clusters in the SU-8 polymer matrix.	16

3.8	Cross-section of the spin-coated nanocomposite film.	17
3.9	TEM images from the various regions of the spin-coated nanocomposite film. These images suggest that nanoparticles have agglomerated in the SU-8 polymer for spin-coated nanocomposite films as well.	17
4.1	Cross-sectional schematic of the capacitor structure in metal insulator metal (MIM) configuration	20
4.2	Equivalent circuit diagram of the dielectric spectroscopy set-up	20
4.3	Dielectric constant of nanocomposite and SU-8 material from 100 KHz to 1.2 MHz. Measured dielectric constant values for the nanocomposite samples are higher than the SU-8 only samples.	21
4.4	Measurement of loss tangent values for nanocomposite and SU-8 only samples.	22

List of Tables

2.1	Summary of important properties of SU-8	5
-----	---	---

Chapter 1

Nanocomposites

1.1 Introduction and Background

Nanomaterials are revolutionizing our world due to their applications in the areas of medicine, energy, environment and communications among others. Due to the unique properties of these materials that arise at nanoscale, advanced technologies as well as improvements in the existing technologies have been made possible. Nanocomposites are a class of nanomaterials with a wide range of properties. These materials are composed of different functional components with at least one component having nanometer dimensions.

Polymer nanocomposites are a subclass of nanocomposites that are obtained by combining fillers (nanoparticles, nanorods, nanoplates) with a polymer matrix. Such materials have been explored for numerous technological applications in the areas of photonics, catalysis, electronics, energy storage and biotechnology [2, 3, 4, 5, 6, 7]. Particularly, polymer nanocomposites containing inorganic fillers like metallic particles dispersed in polymer matrix are of great interest for optical and dielectric applications. Caseri *et al.* [8] utilized gold nanoparticles in order to introduce optical properties such as reversible photochromic behavior, dichroism etc. to the polymer base materials. They also demonstrated that optical properties (e.g., transparency or color) could change upon formation of particle agglomerates. Inorganic metal particles were widely used as fillers for enhancing the dielectric properties of the polymer materials. For example, Pecharroman *et al.* [9] reported a very high dielectric constant of approximately 80,000 at 10 KHz utilizing metallic particles (Ni) in barium titanate matrix. However, these dielectric nanocomposites suffered from various

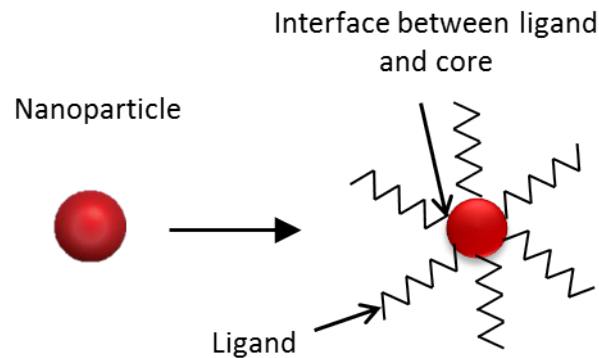


Figure 1.1: Schematic to show a ligand capped nanoparticle surface

limitations such as higher dielectric leakage and reduced electric breakdown strength. These limitations are mainly attributed to nanoparticle agglomeration and inhomogeneous dispersion, which also results in poor processability of films and a high defect density [10]. These findings suggest that physical properties of the composite material are very sensitive to particle dispersion within the nanocomposite. Thus, nanoparticle dispersion control is important. However, studies on investigating and controlling the nanoparticle dispersion are limited.

In the absence of repulsive interactions, nanoparticles tend to agglomerate due to the vander waals attraction between them. Nanoparticles can be prevented from aggregating by grafting polymer brushes or adsorbing surfactant molecules to their surfaces. A schematic of a functionalized nanoparticle surface is shown in Figure 1.1. To improve the dispersion stability of nanoparticles in solvents or polymer matrices, it is essential that the particle surface modification involving polymer surfactant molecules or other modifiers generates a strong repulsion between nanoparticles. In this work, surfactant based ligand molecules have been used for passivating the nanoparticle surface and their success in realizing homogeneous particle dispersion is evaluated.

1.2 Contribution

The thrust of this research is to study the effect of dodecanethiol ligands on the dispersion of metal nanoparticles in the SU-8 polymer matrix. As a model system, gold nanoparticles embedded in SU-8 epoxy resin were selected because of its application potential as a high energy density dielectric material. This is because SU-8 has high breakdown strength and nanoscale conductive fillers can

increase the overall dielectric permittivity of composites on account of the interfacial polarization [11]. Particularly, gold nanoparticles are considered because of their outstanding electrical, optical and thermal properties together with their ability to be synthesized in large volumes with relatively tight size tolerances and passivated with various surface functionalizations. In published literature, polydisperse gold nanoparticles (100 – 300 nm diameter) have been mixed with SU-8, mainly to achieve a conductive nanocomposite material for applications in biomedicine, packaging, sensing and actuation [12]. The report presents the design and fabrication of a novel gold nanoparticle-SU-8 composite material with a focus on investigating the particle distribution in the polymer. This work's secondary thrust is to study the effect of addition of metal nanoparticles on the dielectric properties of the composite material.

The report is structured as follows: After this general introduction, a more detailed introduction of the constituents of the composite material (i.e. dodecanethiol ligand, polymer matrix and fillers) and the experimental techniques used in this study is given in Chapter 2. Chapter 3 describes the fabrication and the material characterization of gold nanoparticle-SU-8 polymer composites. Electrical characterization methods and results are discussed in Chapter 4. Finally, conclusions and future work are presented in Chapter 5.

Chapter 2

Experimental Details

This chapter presents an overview of the materials, experimental methods and the characterization techniques used in this work to synthesize and evaluate the properties of the nanocomposite material.

2.1 Materials

2.1.1 Gold Nanoparticles

In this work, dodecanethiol functionalized gold nanoparticles were embedded inside SU-8 polymer matrix. Nanoparticles of size $(5.6 \pm 0.8 \text{ nm})$ in diameter were purchased in the form of a dried, redispersible powder from Nanocomposix (San Diego, CA). This powder can be redispersed in a variety of organic solvents such as chloroform, toluene, hexane and tetrahydrofuran.

2.1.2 SU-8

SU-8 is a well-established polymer which is commonly used in microfabrication. The physical properties of SU-8 are listed in Table 2.1. It can be inferred that SU-8 has been a very comprehensively investigated material. In addition to the listed properties, SU-8 has good stability at elevated temperatures and resistance to moisture and solvents. Resistance to moisture and solvents basically means that the polymer should not swell or/and dissolve in solvent exposing environments. SU-8 also has unusually high glass transition and degradation temperatures. SU-8 photoresist is

Table 2.1: Summary of important properties of SU-8

Characteristics	Value	Conditions	Reference
Density	1190 Kg/m ³	Raw SU-8 resin	[13]
	1218 Kg/m ³	Fully cross-linked	[14]
Melting point	82°C	Raw SU-8	[15]
Polymer shrinkage	7.5%	Post-baked at 95°C	[16]
Glass transition temperature	50°C	Un-exposed film	[17]
	> 200°C	Fully cross-linked film	[17]
Degradation temperature	380°C	Fully cross-linked	[17]
Volume resistivity	$(1.8 - 2.8) \times 10^{14} \Omega\text{m}$	Hard-baked at 150°C	[18]
Surface resistivity	$(5.1 - 18) \times 10^{14} \Omega\text{m}$	Hard-baked at 150°C	[18]
Relative dielectric constant	4	Post-baked at 100°C; (20 – 40) GHz	[19]
	4.5	at 10MHz	[19]
	5.07	Hard-baked at 150°C, ; 1 MHz	[15]
Loss tangent ($\tan \delta$)	0.14	at 1 THz,	[20]

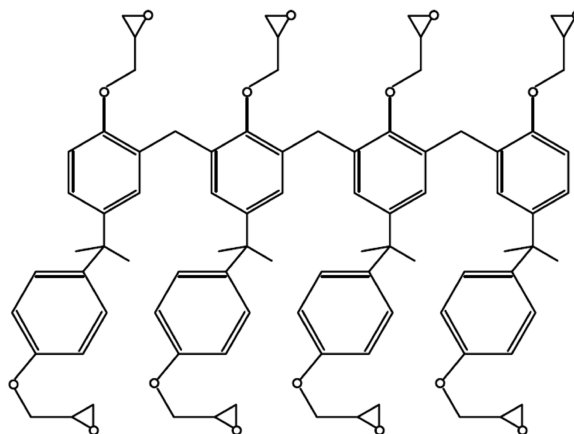


Figure 2.1: Molecular structure of SU-8 monomer. There are eight epoxy groups in the monomer, which justifies the number '8' in the name (SU-8). [21].

composed of Bisphenol A Novolak epoxy oligomer that is dissolved in an appropriate organic solvent and the photoinitiator (usually from triarylsulfonium salts family) to crosslink SU-8. When exposed to light, a photochemical reaction takes place producing an acid which acts as catalyst in the cross-linking reaction. In order for the cross-linking to take place, post exposure bake must be done above the glass transition temperature of SU-8.

The molecular structure of the SU-8 monomer is shown in Figure 2.1. The number '8' in the polymer's name (SU-8) can be assigned to the number of epoxy groups in the oligomer. Bisphenol A Novolak epoxy oligomer also known as EPON Resin SU-8 is commercially available in the granular form and manufactured by Momentive Specialty Chemicals Inc.

2.1.3 Ligands

Gold nanoparticles used in this study were capped with dodecanethiol ligands. Figure 2.2 shows the chemical structure of dodecanethiol. It binds with gold nanoparticle through the formation of a covalent bond between the sulphur and gold atoms (Au-S). Dodecanethiol is a long carbon chain and hence could provide improved stability to nanoparticles.

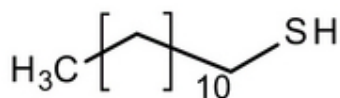


Figure 2.2: Chemical structure of dodecanethiol ligand. Dodecanethiol is a long carbon chain (12 C atoms), with a sulphur atom that binds covalently to the metal nanoparticle core [22].

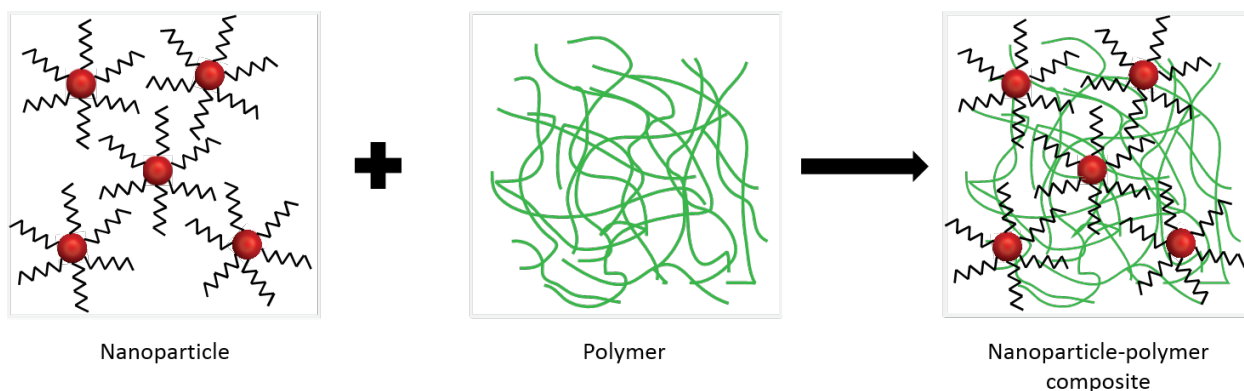


Figure 2.3: *Ex situ* method of polymer nanocomposite material synthesis. In this technique, nanoparticle and polymer components are synthesized separately and then blended to prepare the nanocomposite material.

2.2 Nanocomposite Processing & Characterization Methods

2.2.1 Synthesis methods

Nanocomposite materials are generally synthesized using one of the two methods. The *in situ* method involves the synthesis of one component in the presence of the other. In this method, nanoparticles are synthesized as a sol or dispersed in solution followed by a second step in which monomers are added and polymerized. The second method, *ex situ*, involves blending of pre-made nanoparticles into a pre-synthesized polymer. Unlike *in situ* fabrication, this method provides full synthetic control over both nanoparticles and polymer and has the potential of generating a wide variety of composite materials. In this work, *ex-situ* approach is adopted for the synthesis of nanocomposite material. Figure 2.3 shows a schematic of the synthesis of nanocomposite using *ex situ* method.

In order to synthesize the nanocomposite solution, first the solubility of SU-8 was tested in

various solvents (gamma-butyrolactone (GBL), chloroform, acetone, dimethylformamide (DMF) and benzene. Experimental results showed that SU-8 was completely dissolved in GBL, acetone, chloroform and benzene. Hence, any of these solvents could be used for preparing the polymer solution. We selected chloroform as gold nanoparticles are also dispersible in it. Next, polymer and nanoparticle solutions were prepared separately and mixed under ultrasonication to synthesize the nanocomposite material.

2.2.2 Film Deposition Methods

There are two methods that are mainly used to obtain polymer nanocomposite films. The first method is drop casting that involves placing the nanocomposite solution on the substrate and subsequently, allowing the solvent to evaporate. The second method is spin coating method, in which first, the solution is dropped onto the substrate followed by spinning the substrate at a certain rotation speed for a certain amount of time. Spin casting method results in a much more uniform film thickness than drop casting.

The final film thickness depends on the viscosity of the solution, rotation speed and time. Too high a speed or too long a spin time can result in much faster evaporation of solvent. This can minimize the film thickness but can also result in poor quality films. Too slow a speed or too short a spin time can result in uneven spreading of the solution across the substrate, resulting in non-uniform films. Therefore, a balance must be achieved in order to deposit films well on the substrate.

For the SU-8 based films, after the deposition process ends, a soft bake step is usually performed to ensure that the entire solvent is evaporated followed by UV exposure to induce polymerization which is completed by post exposure bake.

2.2.3 Film Characterization Methods

The thickness of the nanocomposite films were recorded using a stylus contact profilometer (Alpha-Step IQ Surface Profiler). The thickness measurements were made by scanning the stylus across the step from an uncoated substrate area to an area having coated nanocomposite film. Nanocomposite film quality and uniformity was checked using an optical microscope. Scanning Electron Microscopy (SEM), Transmission Electron Microscopy (TEM) and Energy Dispersive X-Ray

Spectroscopy (EDX) techniques were also used to characterize the morphology of nanocomposite films, check nanoparticle dispersion and elemental composition respectively.

Chapter 3

Material Characterization

This chapter presents an evaluation of the properties of gold nanoparticle-polymer composite films using various microscopic characterization techniques.

3.1 Scanning Electron Microscopy

In order to characterize the morphology of polymer nanocomposite films, SEM was used. SEM analysis was performed for various nanocomposite films, synthesized using different deposition methods.

3.1.1 Sample Preparation

For synthesizing nanocomposite films, first a nanocomposite suspension was prepared by mixing gold nanoparticle solution ($40 - 50 \mu\text{g/mL}$) with SU-8 epoxy solution (215mg/mL) in 1 : 4 ratio by volume. Then, samples were prepared under different processing conditions. For sample-1, a 0.1 mL of the resultant nanocomposite suspension was taken and deposited onto a SiO_2 coated Si die by drop casting method, followed by drying under nitrogen for 24 hours. Sample-2 was synthesized similarly except that the deposited film was first UV exposed and then baked in vacuum furnace at $50 - 55^\circ\text{C}$ for 30 minutes. For sample-3, spin coating method was used for depositing the nanocomposite film. A $2 \mu\text{m}$ thick nanocomposite film was prepared by spin coating at 2000 rpm for 30 seconds followed by a soft bake at 95°C for 5 minutes, UV exposure and hard bake at

95°C for 30 minutes to polymerize the SU-8 resin. Figure 3.1 shows the step by step processing for the third sample. All three samples were characterized to check the presence of any voids and cracks through the nanocomposite films. Nanocomposite samples were sputter coated with gold to minimize charging. SEM images were collected using the FEI QUANTA 3D dual beam SEM.

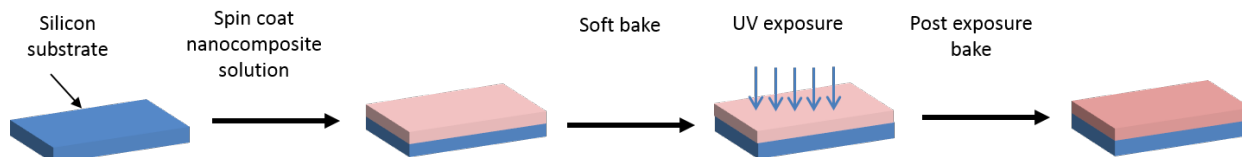


Figure 3.1: Various steps involved in the synthesis of nanocomposite film. After spin coating the nanocomposite film, it is soft-baked to allow evaporation of solvent. Next, it is exposed to UV light for a certain time which depends on the nanocomposite film thickness followed by a hard bake step, to polymerize the SU-8 in the nanocomposite film.

3.1.2 Results

SEM image in Figure 3.2 shows the top surface of the nanocomposite film from sample-1. It can be observed that the film has several micro-bubbles/voids either because the film was dried at room

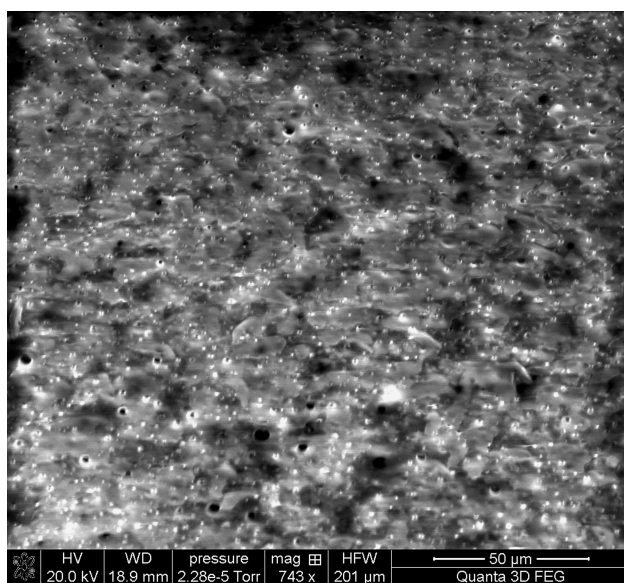


Figure 3.2: SEM image of the top surface of drop-casted nanocomposite film (sample-1). As evident from the presence of microbubbles and voids, a porous nanocomposite film is obtained.

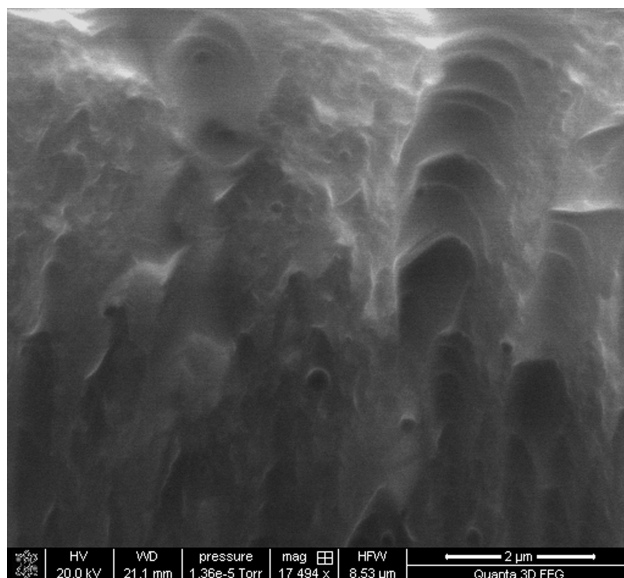


Figure 3.3: Cross-section of the nanocomposite film obtained from sample-2. Unlike sample-1, there are no voids through the nanocomposite film, but a thicker film is obtained ($\sim 65 \mu\text{m}$).

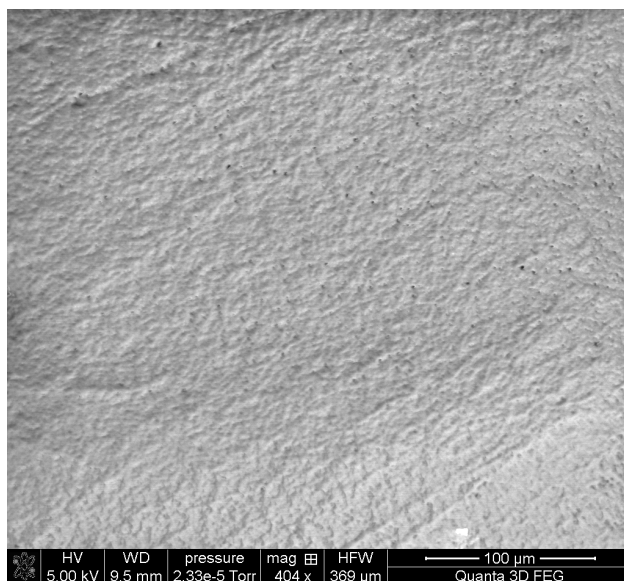


Figure 3.4: SEM image of the top surface of the spin-coated nanocomposite film (sample-3). There are few voids but overall a dense film is obtained.

temperature or cross-linking was not performed. Sample-2 of the nanocomposite material was also characterized using SEM. The cross-section of the nanocomposite film is shown in Figure 3.3. Characterization of the resultant films suggests the absence of voids & defects unlike sample-1.

The film thickness was $65 - 68 \mu\text{m}$. In order to obtain thinner films, spin coating method was used. Figure 3.4 shows the SEM image of the top surface of the spin-coated film i.e. sample-3. It can be observed that a dense film is obtained with no voids or cracks. It is critical to minimize the number of voids and cracks as they affect optimal performance of the nanocomposite material by increasing dielectric leakage and reducing electric breakdown field strength of the nanocomposite dielectric material.

3.2 Energy Dispersive X-Ray Spectroscopy

EDX technique can be used to determine the composition of a specimen. We used the X-ray mapping capability (also known as elemental mapping) of the EDX technique to observe the elemental distribution in the nanocomposite films. In X-ray mapping, positions of specific elements emitting characteristic X-rays within an inspection field can be indicated by unique color. A silicon drift detector of size 20mm^2 was fitted to the FEI SEM for carrying out the EDX analysis.

3.2.1 Sample Preparation

Various samples were prepared by using a nanocomposite solution having higher concentration of nanoparticles in the polymer matrix in comparison to the samples prepared for SEM imaging. EDX analysis for a spin-coated nanocomposite film containing 1 wt% of nanoparticles is illustrated in Figure 3.5.

3.2.2 Results

Figure 3.5 (a), shows the SEM image of the nanocomposite film on which EDX analysis was done. Elemental maps in Figure 3.5 (b,c,d) reveal that carbon (C), oxygen (O) and gold (Au) are the constituent elements of the nanocomposite material. Detection of C and O elements is attributed to the SU-8 polymer. This is evident from the chemical structure of SU-8 as shown earlier in Figure 2.1. Further, Au element is detected because of the addition of gold nanoparticles to the SU-8 polymer. The elemental map of gold (Au), as seen in Figure 3.5 (d), shows a fairly uniform distribution of blue dots/segments. This qualitatively suggests a homogeneous distribution of gold

nanoparticles in the SU-8 matrix. However, it is imperative to perform the TEM analysis to obtain an accurate impression of nanoparticle dispersion in the SU-8 polymer.

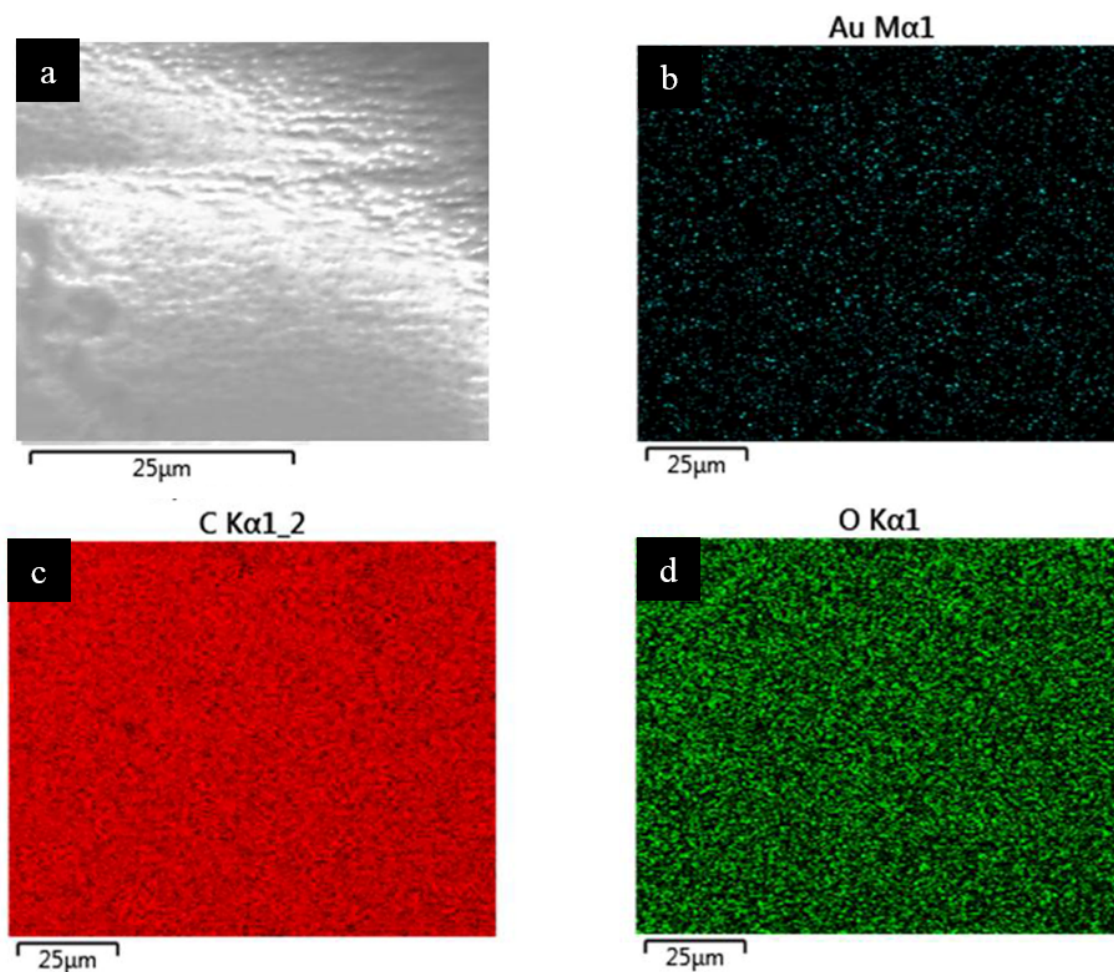


Figure 3.5: EDX analysis of the gold nanoparticle/SU-8 polymer composite material. Figure 3.5 (a) corresponds to the SEM image of the top surface of nanocomposite film. The individual elemental maps are shown in Figure 3.5 (b-d). These maps reveal that C, O and Au are the elemental constituents of the nanocomposite film. Further, the elemental map of Au qualitatively suggests a homogeneous dispersion of gold nanoparticles in the polymer matrix.

3.3 Transmission Electron Microscopy

3.3.1 Sample Preparation

Particle agglomeration and dispersion was studied during the various stages of the nanocomposite synthesis. After dispersing the gold nanoparticle powder in a predetermined amount of chloroform solvent, TEM imaging was done to characterize the particle size and dispersion. A small amount of nanoparticle solution was dropped onto a TEM grid followed by drying and TEM images were collected from the sample.

Both spin-coated and drop-casted nanocomposite films were characterized to study particle agglomeration and dispersion in the SU-8 epoxy. Drop-casted film was synthesized by dropping the nanocomposite solution containing 1 wt% of gold nanoparticles onto an epoxy substrate followed by drying in air for 24 hours. After the evaporation of solvent, resulting film was baked at 95°C for 12 minutes, followed by UV exposure and hard bake at 95°C for 30 minutes. Nanocomposite film was also synthesized by spin-coating the nanocomposite solution at 1500 rpm for 30 seconds followed by soft bake, UV exposure and hard bake step.

In order to characterize the nanoparticle dispersion in the gold nanoparticle-SU-8 polymer composite material, thin slices (50 – 80 nm) of the cross-section of nanocomposite material were prepared by room temperature Reichert ultra microtome (Diatome diamond knife ultra 45°). The nanocomposite sample was cut with a diamond knife attached to a boat in which the cut thin slices float on top of water. A few of these slices were collected and placed onto the TEM grid for imaging. This microtoming procedure was followed for both drop-casted and spin-coated nanocomposite film samples. TEM images were recorded using a FEI Tecnai 12 transmission electron microscope.

3.3.2 Results

Figure 3.6 shows the TEM image of the nanoparticles, obtained prior to mixing them with SU-8 polymer. It shows that nanoparticles are monodispersed and also confirms their size.

TEM was also used for characterizing the nanocomposite films. Figure 3.7 shows the TEM images obtained from the drop-casted nanocomposite films. These images were collected from the various areas of the nanocomposite film. It can be observed in Figures 3.7 (a) and (b) that

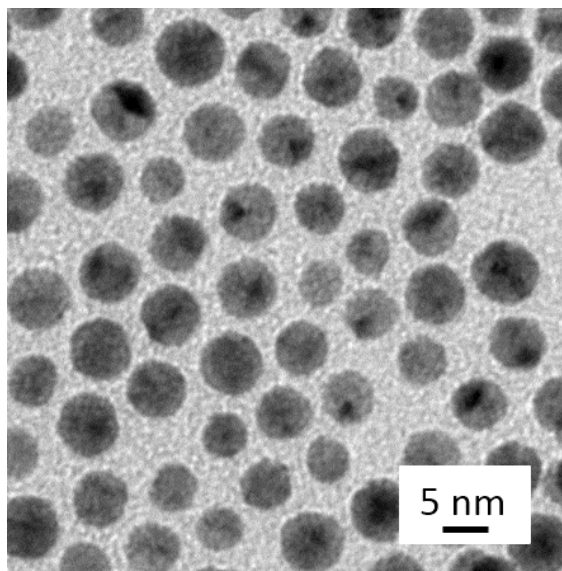


Figure 3.6: TEM image of dodecanethiol functionalized gold nanoparticles

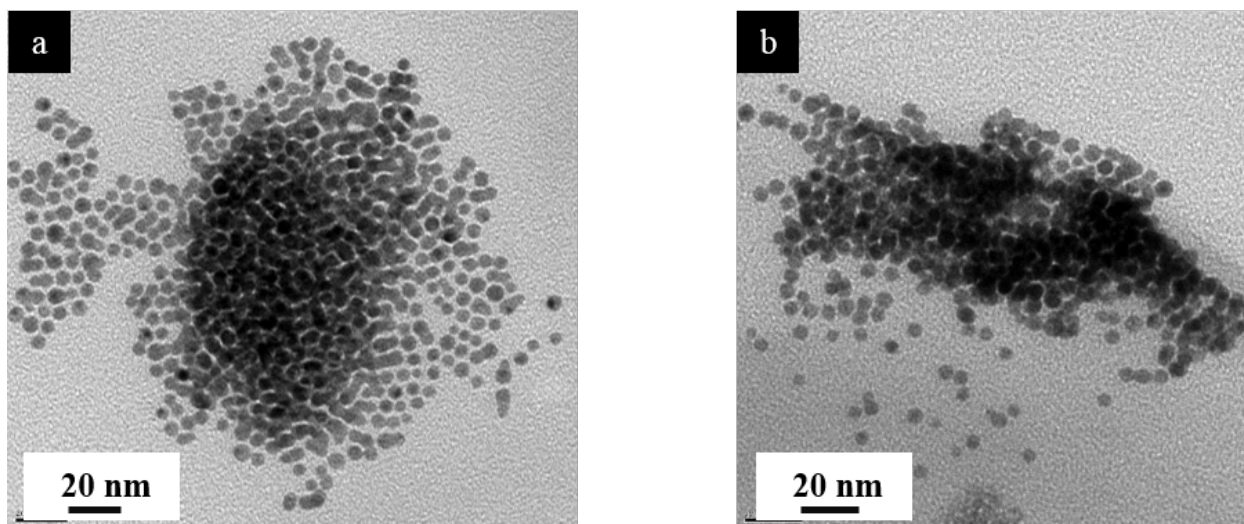


Figure 3.7: TEM analysis of the drop-casted nanocomposite films. These images show that nanoparticles are dispersed in form of clusters in the SU-8 polymer matrix.

nanoparticles have agglomerated in clusters throughout the nanocomposite film. Moreover, the nanoparticle distribution is inhomogeneous. Therefore, a uniform dispersion of nanoparticles is not achieved. This behavior of nanoparticles could be either due to the lack of compatibility between ligand and polymer phases or due to stripping off the ligands from nanoparticle surface during ultrasonication or thermal annealing of polymer nanocomposite films.

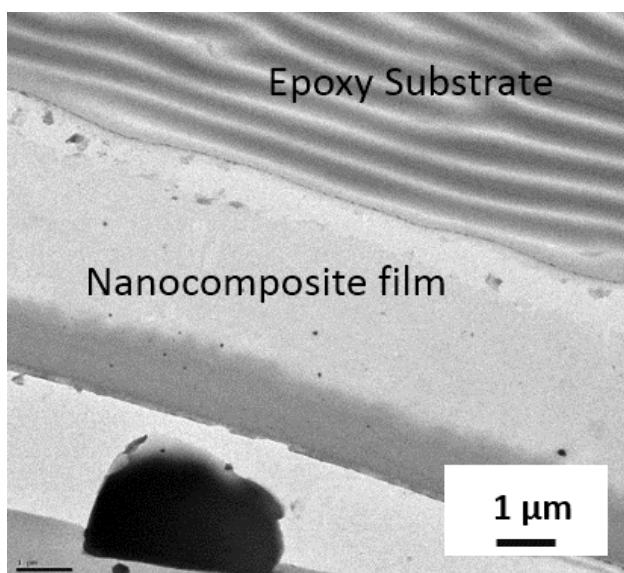


Figure 3.8: Cross-section of the spin-coated nanocomposite film.

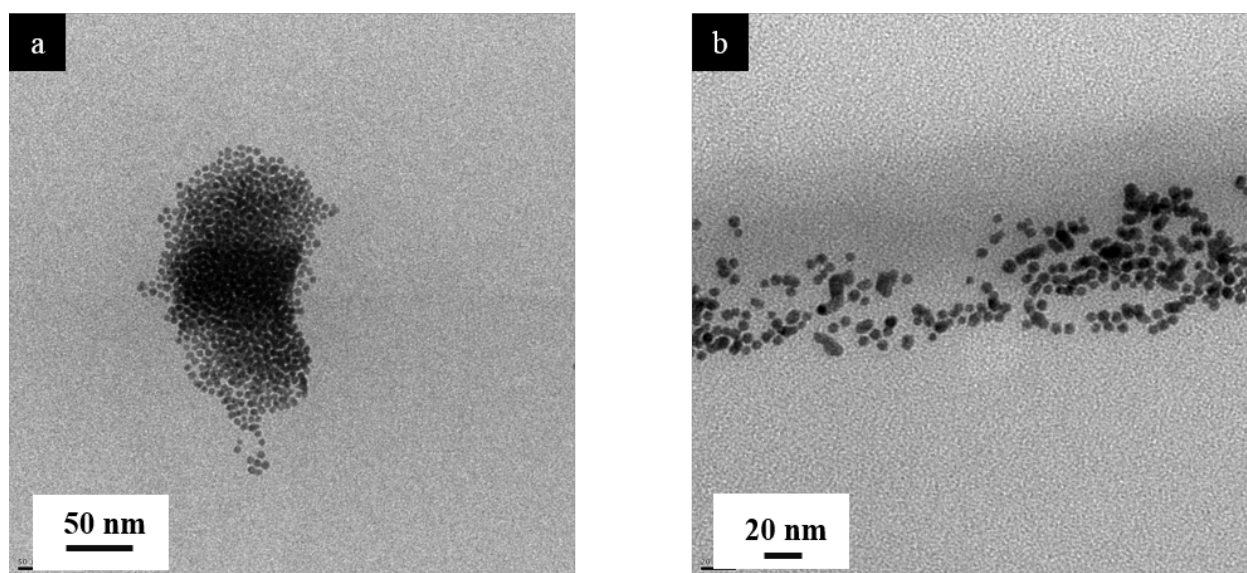


Figure 3.9: TEM images from the various regions of the spin-coated nanocomposite film. These images suggest that nanoparticles have agglomerated in the SU-8 polymer for spin-coated nanocomposite films as well.

Figure 3.8 shows a TEM image of the cross-section of the spin-coated nanocomposite film. The film is resting on an epoxy substrate. It can be inferred that the thickness of the film is on the order of micrometers. In order to observe nanoparticle dispersion, images were captured in higher magnifications from different areas of the nanocomposite film. Figures 3.9 (a) and (b) show that an

inhomogeneous dispersion of nanoparticle clusters is achieved in the spin-coated nanocomposite films. This is similar to the drop-casting case.

3.4 Discussion

Material characterization of the nanocomposite material revealed the film morphology and the state of nanoparticle dispersion. Nanocomposite films of low thickness and high quality can be successfully produced using the spin-coating method in conjunction with the appropriate SU-8 processing conditions. However, nanoparticle agglomeration and dispersion in nanocomposite still needs to be improved since, dodecanethiol ligands have remained ineffective in preventing particle aggregation. Other surface functionalizations/ligands can be tested to improve particle dispersion and agglomeration.

Chapter 4

Electrical Characterization

4.1 Device Fabrication

In order to measure the dielectric properties of the nanocomposite material, prototype capacitor devices were fabricated in a metal insulator metal (MIM) configuration. First, a 100 nm thick layer of SiO_2 was deposited onto a silicon die of size $10\text{ mm} \times 20\text{ mm}$ using plasma enhanced chemical vapor deposition (PECVD) method. Next, a 200 nm thick layer of aluminum was sputtered onto the SiO_2 layer, which acts as the bottom electrode, followed by the spin-coating and polymerization of the nanocomposite film (1 wt% nanoparticle content) using the procedure mentioned in Section 3.1. Finally, 100 nm thick gold electrodes of size 2 mm in diameter were evaporated through a shadow mask, using an electron beam evaporator (Edwards EB3 electron beam evaporator) onto the nanocomposite film. Figure 4.1 shows the layout of the capacitor device. In order to compare the dielectric performance of gold nanoparticle-SU-8 polymer nanocomposite with the SU-8 polymer, capacitor devices having SU-8 as dielectric layer were also fabricated in a similar manner. Both SU-8 and nanocomposite dielectric films had a film thickness of $2\ \mu\text{m}$ approximately.

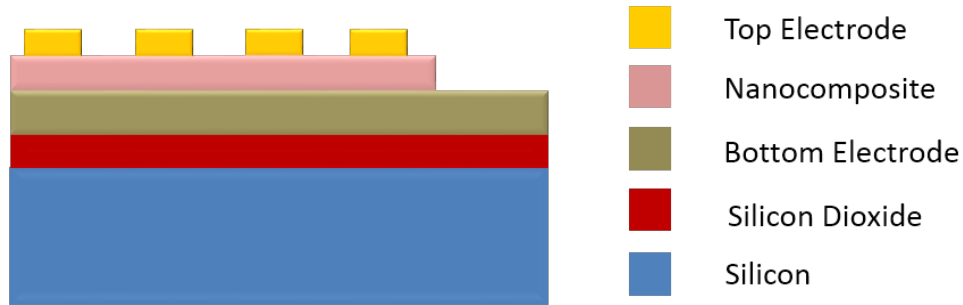


Figure 4.1: Cross-sectional schematic of the capacitor structure in metal insulator metal (MIM) configuration

4.2 Measurements & Results

4.2.1 Dielectric Spectroscopy

The electric permittivity of a material is constant in a DC field in the absence of dielectric saturation. Under an AC field, the permittivity of a material strongly depends on the frequency of the applied electric field and can be expressed in the form of a complex number with a real part ϵ' and an imaginary part ϵ'' . The ratio of the imaginary part to the real part of permittivity, ϵ''/ϵ' , is defined as the dissipation factor (DF) which is also known as the loss tangent ($\tan \delta$) because it is related to the dielectric loss.

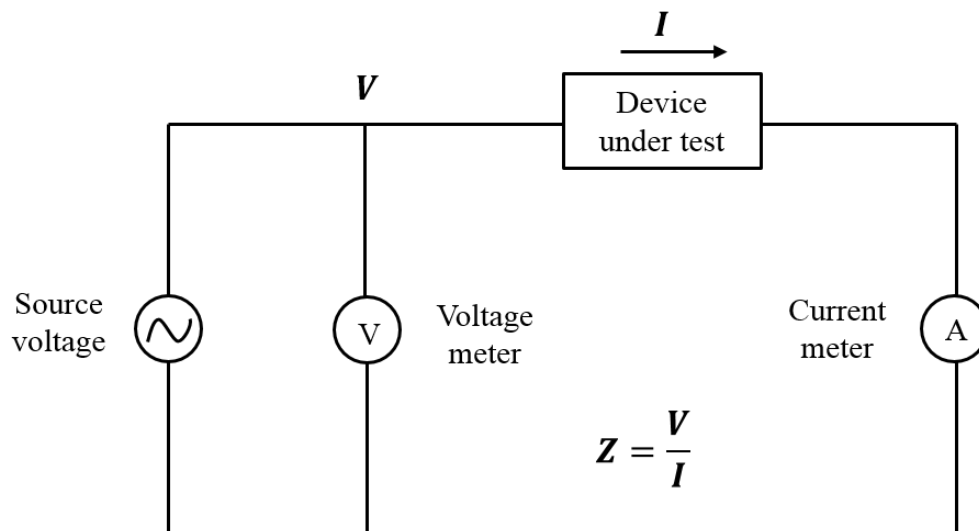


Figure 4.2: Equivalent circuit diagram of the dielectric spectroscopy set-up

Electrical measurements were performed using a probe station (Signatone, model H100) with a blunt tungsten probe tip to minimize mechanical damage to the soft organic nanocomposite films. Characterization of both nanocomposite and polymer only capacitor devices was done in an ambient atmosphere.

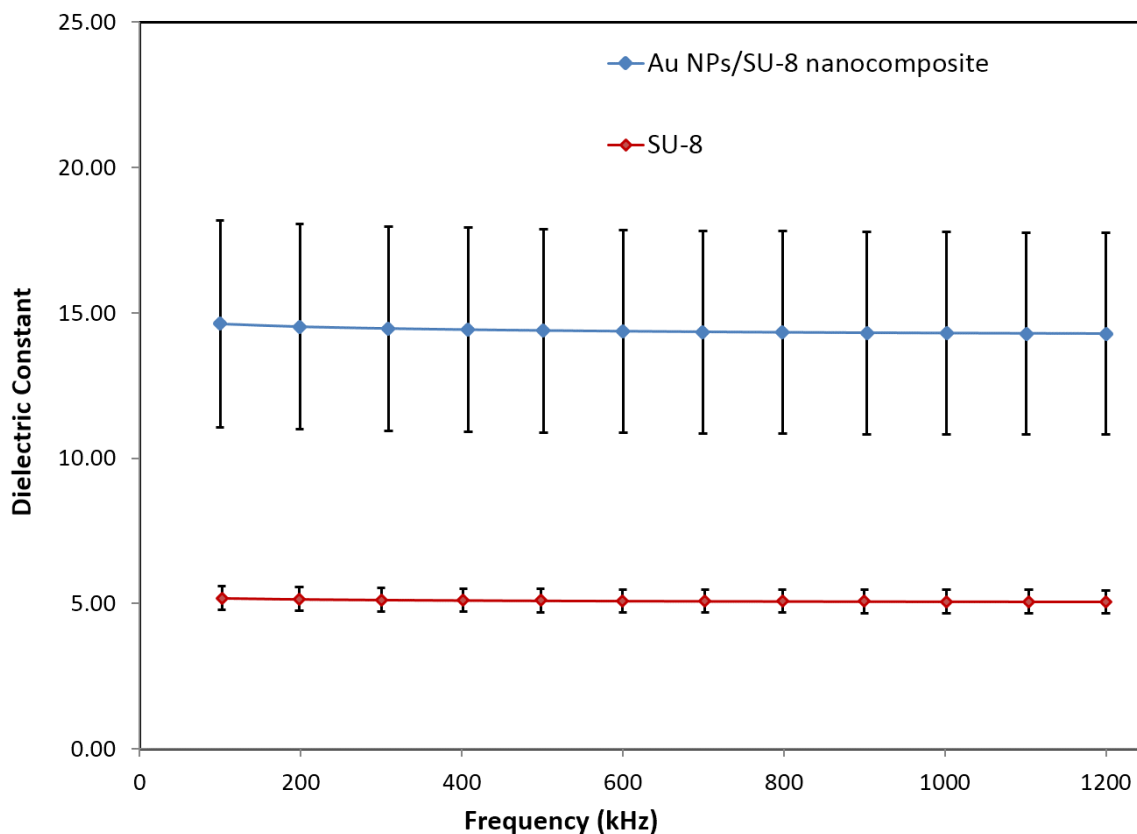


Figure 4.3: Dielectric constant of nanocomposite and SU-8 material from 100KHz to 1.2MHz. Measured dielectric constant values for the nanocomposite samples are higher than the SU-8 only samples.

Agilent's E4980A precision LCR meter with a frequency range from 20Hz to 1.2MHz was used for measuring the capacitance and loss tangent of the nanoparticle-polymer composite films, and the measured impedance was analyzed to calculate the real and imaginary parts of permittivity. Figure 4.2 shows a circuit diagram of the capacitance measurement set-up. Measurement errors could arise due to the stray admittance and residual impedance of the test fixture used. In order to eliminate the measurement errors, calibration was performed in the open and short circuit condi-

tions. The first step to perform a correction on the test system is to apply a short across the probes, typically by setting the two probe heads down on the same contact pad. Then, the capacitance meter measures the impedance value, and stores it as the residual short impedance. The next step is to lift the probes, keeping them in an orientation that approximates where they will be when the actual device is measured. Then the capacitance meter measures the value, and stores that as the residual open impedance. After performing the calibration, dielectric spectra were recorded from 20 Hz to 1 MHz with a probing voltage of $1 V_{\text{rms}}$ under no DC bias.

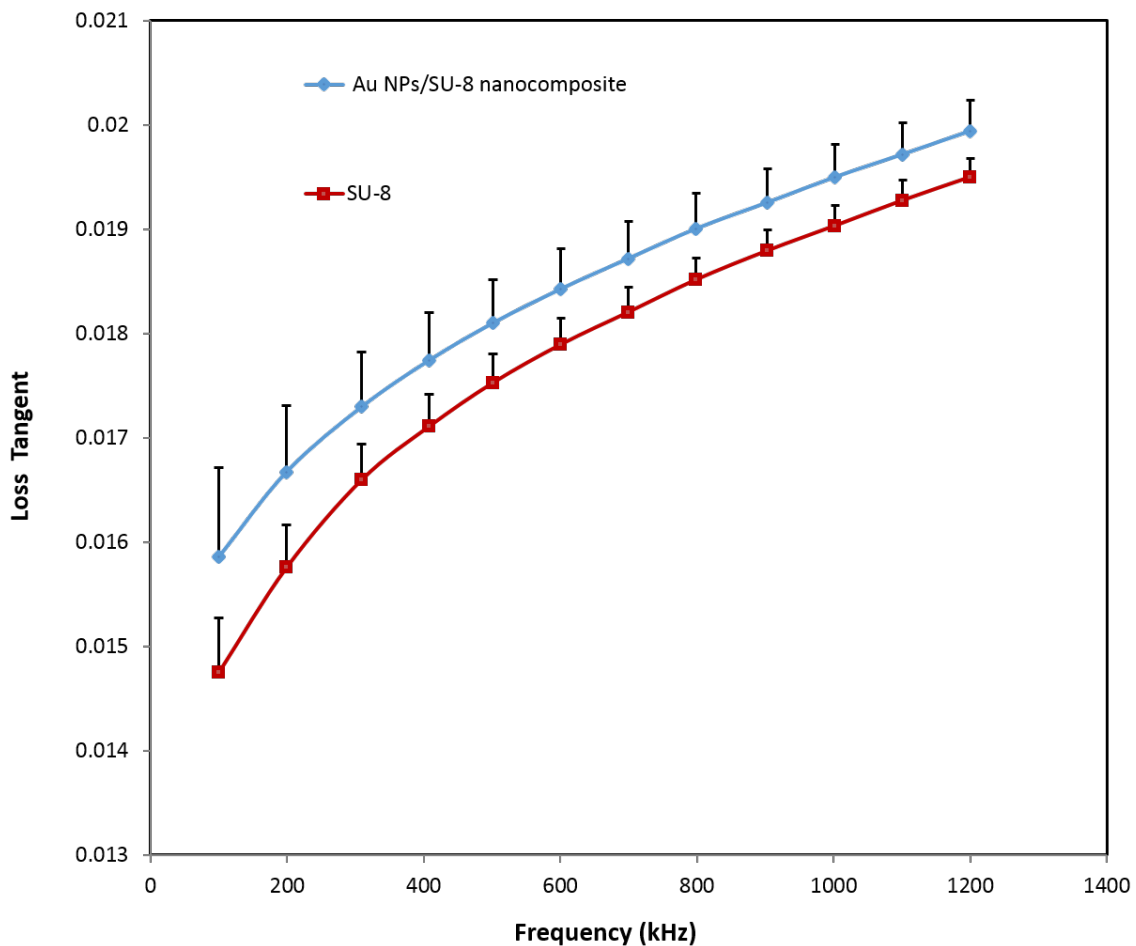


Figure 4.4: Measurement of loss tangent values for nanocomposite and SU-8 only samples.

Four samples each of nanocomposite and SU-8 only capacitors were tested to determine the dielectric constant and loss tangent values. In Figure 4.3, average dielectric constant values were plotted against frequency with the error bars showing one standard deviation from the mean di-

electric constant obtained from various samples. Figure 4.3 shows that the dielectric constant of the nanocomposite and the polymer-only samples remains constant with the frequency. Also, it is clearly demonstrated that gold-SU-8 nanocomposite samples have higher dielectric constant than the polymer only samples. Further improvement in the dielectric constant of the nanocomposite material could be achieved by increasing the volume fraction of nanoparticles in the polymer.

Figure 4.4 shows the average loss tangent values for the nanocomposite and SU-8 only capacitors. Error bars represent one positive standard deviation from the average loss tangent value. It can be observed that the average loss tangent for nanocomposite capacitors is higher than the SU-8 only capacitors. This is expected due to the presence of metallic fillers in the SU-8 matrix for nanocomposite capacitors. However, the absolute value of loss tangent is still really low. This implies that dielectric leakage is quite low.

4.3 Discussion

Dielectric constant measurements demonstrated that the addition of gold nanoparticles to the SU-8 polymer matrix resulted in the enhancement of dielectric constant, which can be further improved by increasing the particle concentration in the polymer. However, particle agglomeration and dispersion needs to be controlled in order to achieve optimal performance as nanocomposite materials containing particle aggregates would suffer from higher dielectric leakage and reduced breakdown field strength with increase in the particle concentration.

Chapter 5

Conclusion and Future Work

5.1 Conclusion

This work has demonstrated the synthesis and characterization of a novel gold nanoparticle-SU-8 based composite material. Agglomeration and dispersion of gold nanoparticles in the SU-8 polymer matrix was discussed in detail. Particle agglomeration and inhomogeneous dispersion revealed the lack of compatibility between the particle ligands (dodecanethiol) and polymer phase (SU-8). A film casting procedure was developed to obtain void and crack free nanocomposite films. Measured dielectric properties of the polymer composite material (1 wt% nanoparticle content) showed a three time enhancement in the effective relative permittivity relative to the polymer material. Electrical characterization results shows that a significant increase in the dielectric constant can be expected for nanocomposites containing higher volume fraction of nanoparticles.

5.2 Future Work

There are several technical challenges worth investigating to optimize the performance of the gold nanoparticle-SU-8 polymer composite dielectric material. A detailed analysis on the influence of various surface functionalizations on gold nanoparticle dispersion and aggregation can be performed to identify compatible nanoparticle ligands, which can ultimately aid in achieving homogeneous particle dispersion. Moreover, for a particular ligand type (for example, dodecanethiol), the effect of areal density of ligand molecules on nanoparticle dispersion can also be studied. These

analyses could be helpful in identifying control parameters that can be adjusted to achieve the desired nanoparticle dispersion. Performance of the nanocomposite materials having homogeneous particle dispersion can be compared to the ones with inhomogeneous dispersion to quantify the influence of particle dispersion on dielectric properties.

References

- [1] Michael E Mackay et al. “General strategies for nanoparticle dispersion”. In: *Science* 311.5768 (2006), pp. 1740–1743.
- [2] Keun Hyung Lee et al. “Dielectric properties of barium titanate supramolecular nanocomposites”. In: *Nanoscale* 6.7 (2014), pp. 3526–3531.
- [3] GM Ouyang, KY Wang, and XY Chen. “Enhanced electro-mechanical performance of TiO₂ nano-particle modified polydimethylsiloxane (PDMS) as electroactive polymers”. In: *Solid-State Sensors, Actuators and Microsystems Conference (TRANSDUCERS), 2011 16th International*. IEEE. 2011, pp. 614–617.
- [4] Tetsuji Inui et al. “High-dielectric paper composite consisting of cellulose nanofiber and silver nanowire”. In: *Nanotechnology (IEEE-NANO), 2014 IEEE 14th International Conference on*. IEEE. 2014, pp. 470–473.
- [5] Dong Kee Yi, Su Seong Lee, and Jackie Y Ying. “Synthesis and applications of magnetic nanocomposite catalysts”. In: *Chemistry of materials* 18.10 (2006), pp. 2459–2461.
- [6] P Markondeya Raj et al. “Tunable and miniaturized RF components with nanocomposite and nanolayered dielectrics”. In: *Nanotechnology (IEEE-NANO), 2014 IEEE 14th International Conference on*. IEEE. 2014, pp. 27–31.
- [7] Xin Li et al. “Electromagnetic functionalized and core-shell micro/nanostructured polypyrrole composites”. In: *The Journal of Physical Chemistry B* 110.30 (2006), pp. 14623–14626.
- [8] Walter Caseri. “Inorganic nanoparticles as optically effective additives for polymers”. In: *Chemical Engineering Communications* 196.5 (2008), pp. 549–572.

- [9] Carlos Pecharroman et al. “New Percolative BaTiO₃-Ni Composites with a High and Frequency-Independent Dielectric Constant(ϵ_r 80000)”. In: *Advanced Materials* 13.20 (2001), p. 1541.
- [10] Philseok Kim et al. “High energy density nanocomposites based on surface-modified BaTiO₃ and a ferroelectric polymer”. In: *ACS nano* 3.9 (2009), pp. 2581–2592.
- [11] C-W Nan, Y Shen, and Jing Ma. “Physical properties of composites near percolation”. In: *Annual Review of Materials Research* 40 (2010), pp. 131–151.
- [12] H Chiamori et al. “Suspension of Nanoparticles in SU-8 and Characterization of Nanocomposite Properties”. In: *ENS 2005*. TIMA Editions. 2005, pp. 131–136.
- [13] I Roch et al. “Fabrication and characterization of an SU-8 gripper actuated by a shape memory alloy thin film”. In: *Journal of Micromechanics and Microengineering* 13.2 (2003), p. 330.
- [14] R Feng and RJ Farris. “The characterization of thermal and elastic constants for an epoxy photoresist SU8 coating”. In: *Journal of materials science* 37.22 (2002), pp. 4793–4799.
- [15] Hexion. *EPON Resin SU-8, Technical Data Sheet*.
- [16] LJ Guerin et al. “Simple and low cost fabrication of embedded microchannels by using a new thick-film photoplastic”. In: *Transducers*. Vol. 97. 1997, pp. 1419–1422.
- [17] KY Lee et al. “Micromachining applications of a high resolution ultrathick photoresist”. In: *Journal of Vacuum Science & Technology B* 13.6 (1995), pp. 3012–3016.
- [18] Microchem. *SU-8 table of properties*. URL: <http://www.microchem.com/pdf/SU-8-table-of-properties.pdf>.
- [19] JR Thorpe, DP Steenson, and RE Miles. “High frequency transmission line using micromachined polymer dielectric”. In: *Electronics Letters* 34.12 (1998), pp. 1237–1238.
- [20] S Arscott et al. “Terahertz time-domain spectroscopy of films fabricated from SU-8”. In: *Electronics Letters* 35.3 (1999), pp. 243–244.

- [21] Anju Toor, Jim C Cheng, and Albert P Pisano. “Synthesis and characterization of gold nanoparticle/SU-8 polymer based nanocomposite”. In: *Nano/Micro Engineered and Molecular Systems (NEMS), 2014 9th IEEE International Conference on*. IEEE. 2014, pp. 664–668.
- [22] Merckmillipore. *Dodecanethiol datasheet*. URL: http://www.merckmillipore.com/INTL/en/product/chemicals,MDA_CHEM-820544.